Trends in Snowfall versus Rainfall in the Western United States

NOAH KNOWLES

U.S. Geological Survey, Menlo Park, California

MICHAEL D. DETTINGER AND DANIEL R. CAYAN

U.S. Geological Survey, Menlo Park, and Scripps Institution of Oceanography, University of California, San Diego, La Jolla, California

(Manuscript received 29 April 2005, in final form 21 November 2005)

ABSTRACT

The water resources of the western United States depend heavily on snowpack to store part of the wintertime precipitation into the drier summer months. A well-documented shift toward earlier runoff in recent decades has been attributed to 1) more precipitation falling as rain instead of snow and 2) earlier snowmelt. The present study addresses the former, documenting a regional trend toward smaller ratios of winter-total snowfall water equivalent (SFE) to winter-total precipitation (*P*) during the period 1949–2004.

The trends toward reduced SFE are a response to warming across the region, with the most significant reductions occurring where winter wet-day minimum temperatures, averaged over the study period, were warmer than −5°C. Most SFE reductions were associated with winter wet-day temperature increases between 0° and +3°C over the study period. Warmings larger than this occurred mainly at sites where the mean temperatures were cool enough that the precipitation form was less susceptible to warming trends.

The trends toward reduced SFE/*P* ratios were most pronounced in March regionwide and in January near the West Coast, corresponding to widespread warming in these months. While mean temperatures in March were sufficiently high to allow the warming trend to produce SFE/*P* declines across the study region, mean January temperatures were cooler, with the result that January SFE/*P* impacts were restricted to the lower elevations near the West Coast.

Extending the analysis back to 1920 shows that although the trends presented here may be partially attributable to interdecadal climate variability associated with the Pacific decadal oscillation, they also appear to result from still longer-term climate shifts.

1. Introduction

One of the most common, and common sense, projections of the impact of global warming on the western United States is that warming will reduce the volumes and persistence of snowpacks across the region (e.g., Gleick 1987; Lettenmeier and Gan 1990; Dettinger et al. 2004; Knowles and Cayan 2004; Stewart et al. 2004). Warming in the western states is expected to reduce the fraction of precipitation that falls as snow rather than rain and hasten the onset of snowmelt once snowpacks have formed.

In this context, recent observations in many rivers of the mountainous western United States and Canada indicate a tendency for streamflow from snow-dominated basins to arrive progressively earlier in recent decades in response to large-scale warming (Roos 1991; Dettinger and Cayan 1995; Cayan et al. 2001). Widespread trends toward less winter's end (April) snowpack water content have also been reported (Mote 2003; Mote et al. 2005). Trends in the dates of onset of rapid snowmelt runoff in spring (Cayan et al. 2001; Stewart et al. 2005) indicate that an important part of the changes in runoff timing has been the earlier onset of springtime snowmelt across the region, but the possible contribution of shifts toward more rainfall and less snowfall has received less attention to date. In the northeastern states, trends toward decreases in the fraction of precipitation as snowfall have already been documented (Huntington et al. 2004). To better understand the nature of the observed changes in snowpack and streamflow timing in the West, historical changes in the relative contributions of rainfall and snowfall are assessed here.

Corresponding author address: Noah Knowles, U.S. Geological Survey, MS 496, 345 Middlefield Rd., Menlo Park, CA 94025.
E-mail: nknowles@usgs.gov

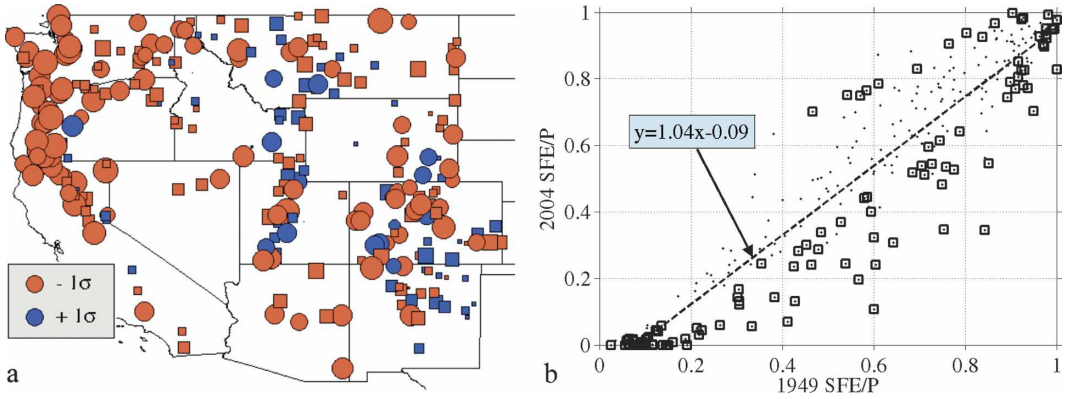

FIG. 1. (a) Trends in fraction of winter (Nov–Mar) precipitation falling on snowy days (SFE/*P*), 1949–2004: red indicates decreasing snowfall fractions; symbol radius is proportional to study period changes, measured in standard deviations of the detrended time series as indicated; circles indicate high trend significance ($p < 0.05$), and squares indicate lower trend significance. (b) The WY2004 winter SFE/*P* vs WY1949 winter SFE/*P*, with significant SFE/*P* trends highlighted with squares. Dashed line is the least squares fit to all data points.

Western warming trends historically have been (and presumably will continue to be) marked by strong seasonal and geographic patterns (e.g., Diaz and Quayle 1980; Dettinger et al. 1995; Cayan et al. 2001). Because of the general wintertime maximum of snowfall and precipitation in the region, contributions of snow to western precipitation are likely to be most affected by wintertime (November–March) temperatures, whereas changes in onset of snowmelt (once snow is on the ground) are more likely to be sensitive to springtime temperatures. Thus, snow deposition and snowmelt are expected to be differently sensitive to warming trends in different seasons, and the warming trends associated with snowfall and snowmelt changes may be distinguishable by differences in their geographic patterns and rates of change. Much work has been accomplished in mapping trends in snowmelt response; this study documents a parallel set of trends that has changed the relative contributions of snowfall to western precipitation.

In section 2, the data used and the methods applied are discussed, and the robustness of the approach is addressed. In section 3a, trends in winter precipitation form are presented, and in section 3b, the influence of temperature on these trends is examined. In section 3c, the monthly patterns underlying the seasonal trends are presented. In section 3d, the role of climate variability in generating trends in precipitation form is investigated. Finally, the main results are summarized in section 4, and their implications discussed.

2. Data and methods

The measure of snowfall that will be used in this study is the snowfall liquid water equivalent (SFE), defined as the precipitation totals on days for which newly fallen snow was recorded. These data and the temperature data used in this study were derived from the historical Summary of the Day (SOD) observations from cooperative weather stations in the 11 westernmost states of the conterminous United States (Fig. 1), obtained from the National Climatic Data Center. The observations used here comprise daily snowfall depth (*S*, actual depth as opposed to liquid equivalent), precipitation (*P*, regardless of form), and maximum (TMAX) and minimum (TMIN) surface air temperature, from October 1948 to September 2004. Because *S* is not a reliable proxy for snowfall liquid equivalent since snow density can vary significantly, and because *P* observations have no associated data flags indicating the precipitation form (i.e., solid, liquid, or mixed), in this study, a nonzero value of snowfall depth (*S*) is used to assign a solid form to any measured precipitation (*P*), thereby estimating snowfall water equivalent (SFE).

Precipitation and snowfall totals were recorded at 1653 stations during some or all of this period; temperatures were recorded at 1517 stations. Emulating the approach developed by Huntington et al. (2004) for a similar analysis in the northeastern United States, the records of precipitation and snowfall at the western stations were culled according to the following sequential steps.

1) Any cool season during which precipitation or snowfall data were missing for 10 or more days between November and March was considered incomplete and was excluded from the analysis.
2) Any station that was missing >50% of its November–March daily observations in any given 10-yr period was excluded.

3) Any station at which the mean winter snowfall total (described here by the November–March sums of daily snowfall water equivalents, SFE, described below) was less than 25 mm was excluded.

This study focused on a winter season, defined here as November–March, because, on average over all the stations, 80% of snowfall occurred during that interval. The analyses below were repeated using the period October–May, which accounted for 98% of snowfall aggregated over all stations and greater than 90% of snowfall at every individual station. No substantial changes in the results were obtained by using this longer season, except that fewer stations survived the completeness tests and the relative contributions of snow to overall precipitation were numerically smaller due to the inclusion of the warmer months.

Steps 1 and 2 were also applied to TMAX and TMIN. These criteria ensure that the data analyzed here are sufficiently serially complete that seasonal averages or totals, trends, and other long-term patterns in temperature and snowfall can be reliably calculated without undue interference from sampling errors and seasonal effects. This culling retained 261 stations with precipitation and snowfall, 634 stations that contained temperature, and 207 stations that contained temperature, precipitation, and snowfall. The analyses presented here used the largest appropriate dataset in each case (i.e., joint analysis of temperature and precipitation used 207 stations, while analysis of temperature alone used all 634 stations).

To further ensure the robustness of the results, the remaining data were examined for trends in the number of days with missing data, in the average date of the missing values each winter, and in the standard deviation of the dates of missing values each winter. Significant trends were found in the number of missing days at many stations, and the analysis presented below was repeated with those stations excluded. The analysis was also repeated using more stringent criteria in steps 1 and 2 above—thresholds of 3 days in step 1 and 25% in step 2. In both cases, the conclusions of this analysis were unchanged, albeit with fewer data points. Finally, repeating the analysis without the Great Plains stations (described in section 3b) did not change the findings of this paper.

The depth of newly fallen snow (S) is recorded each day by cooperative observers using a variety of methods, including simple measuring sticks; snow boards, which are wiped clean after each measurement; and tall snow stakes where large snow accumulations occur. Liquid (equivalent) precipitation depth (P) is typically measured with precipitation gauges. The daily accumulated precipitation is either melted and the liquid depth measured, or, in the case of recording gauges, the precipitation is weighed (National Weather Service 1989).

A potential problem with the use of precipitation gauge measurements for comparing snowfall to total precipitation is that the catch efficiency is typically lower for snow than for rain. The influence on the results presented below of this phenomenon of undercatch was estimated by assuming all solid precipitation was associated with a gauge efficiency of 50%, and all liquid precipitation with an efficiency of 90%, then repeating the analyses of this study. This difference in catch efficiencies represents an upper extreme among previous studies' findings for the gauge types and conditions found in the western United States (Yang et al. 1998; Groisman and Legates 1994). The results suggest that undercatch had relatively little effect on the trends reported here, and, if anything, resulted in an underestimation of trends in the SFE/P ratio and SFE. A more rigorous treatment of these effects was not possible due to the paucity of catch efficiency data for the individual stations studied.

Although they have been selected to have recorded snowfall (criterion 3 above), the SOD station subset is generally representative of lower and middle elevations. For example, the median elevation from the snow/precipitation SOD subset is 1380 m, while the median elevation of snow pillows in the same region is 2380 m. However, as will be brought out in the results, the elevational distribution of the SOD stations is well situated to record changes in precipitation form from relatively modest climate fluctuations or changes. This is because elevations below 2000 m are nearer to freezing and thus more sensitive to temperature changes than are the higher, colder elevations that are generally characteristic of snow courses and snow pillows.

In a relatively small number of cases, P was not measured directly, but was estimated on snowy days by applying some fixed multiplier (corresponding to an assumed snow density) to the depth of snow (S), typically 0.1 (e.g., U.S. Department of Agriculture Weather Bureau 1935). To test for this practice and to determine whether such cases adversely affect the results presented here, the precipitation and snowfall depth (S) data were examined for overabundances of integer values of the ratio S/P. The most frequently reported integer ratio was 10, which was reported (within a roundoff tolerance of 0.05) on an average of 0.4% of snowy days, followed by 20 on 0.1% of the snowy days. The station with the largest percentage of snowy days for which $S/P = 10$ was a site in Montana with 6%. Removing those stations (36 stations out of 261) whose

percentage of November–March snowy days with $S/P = 10$ was greater than 2% from the analysis resulted in no substantial changes to this paper's conclusions.

In this study, the liquid water equivalent of newly fallen snow on each day (SFE, not to be confused with SWE, a common acronym for the liquid equivalent of the season-to-date's accumulated snowpack) is defined as equal to P on days when $S > 0$, and equal to zero when $S = 0$. While this definition can overstate the amount of precipitation as snowfall (since precipitation on some days is a mixture of snow and rain), it avoids overreliance on the reported snowfall amounts, which are notoriously unreliable and observer dependent. Additionally, overestimation of the SFE/P ratio on mixed-form days will underestimate the contributions of those days (or trends in the number of those days) to trends in seasonally totaled SFE/P, so that our choice results in, if anything, the underestimation of the magnitude of trends in snowfall (as a fraction of total precipitation). Our definition also does not distinguish between rainfall and snowfall that melts completely on the same day it falls (before it can be measured).

The sums of SFE and P over all days with data in each winter (after the culling process described above) form time series of winter and monthly totals of SFE and P, from which winter and monthly ratios SFE/P, the fraction of precipitation falling as snow, were calculated. A Kendall's tau nonparametric trend analysis (Kendall 1938) was performed on each time series. Additionally, a least squares regression line was fitted to each time series to estimate the magnitudes of changes over the 56-yr study period, and each trend was further quantified in terms of standard deviations of the detrended yearly time series. In the rare cases when a linear fit produced (physically impossible) negative values, only the positive segment of the fit was used to determine the magnitudes of the SFE, P, or SFE/P changes. Similar procedures were applied to winter-averaged temperatures.

The analyses below were initially performed with a dataset restricted to sites in the U.S. Historical Climatology Network daily collection (HCN/D; Easterling et al. 1999), as in Huntington et al. (2004). That dataset was selected from among the SOD sites according to various quality assurance criteria, in order (where possible) to minimize such data quality concerns as inconsistencies of daily maximum and minimum temperature measurement times instrument changes, and heat island effects. However, in order to achieve the desired spatial coverage in the HCN/D dataset (compared to the original HCN monthly dataset), these criteria were not strictly applied, nor were any corrections for nonclimatic effects applied as they were in the larger monthly HCN dataset (Easterling et al. 1996). When steps 1–3 were applied to the HCN/D subset for the western United States, the number of stations that survived was barely sufficient to discern spatial patterns in the data. To include a fuller network of stations, the present analysis applied the completeness criteria, as described above, to the full SOD dataset rather than to the HCN/D subset. This strict culling of a larger initial dataset yielded enough stations to discern spatial patterns. Similar patterns were evident in trend analyses of the HCN/D dataset (not shown here), but with much more sparsely populated maps. This replication of results when a higher quality but sparser dataset was analyzed gives us confidence that the trends and patterns reported here are climatic in their origins, even though nonclimatic effects such as heat island bias (Karl et al. 1988), measurement time changes, and instrumentation changes have not been corrected for in the (more populous) dataset used in this paper.

Most of the analyses presented are from the primary precipitation, snowfall depth, and temperature datasets taken from 1949 to 2004. However, to obtain a better understanding of the temporal variability of the snowfall fraction and its linkage to temperature, some analyses in Section 3d use two smaller subsets of stations beginning in 1930 and 1920.

3. Results

a. Seasonal SFE/P trends

The fraction of winter precipitation falling on snowy days (SFE/P) trended toward smaller values during water years (WY) 1949–2004 at 192 (74%) of the 261 SOD sites analyzed (Fig. 1a) and increased at the other 69 sites. Many of these trends did not rise to the level of statistical significance ($p < 0.05$, under the standard Student's t test that applies to Kendall's tau analyses); however, of the sites with trends that did rise to this level, the snowfall fraction decreased at 94 sites (87%) and increased at only 14. Trends toward decreasing snowfall fractions were strongest (in terms of standard deviations of the detrended yearly ratios) at the lower-elevation sites in the Sierra Nevada and the Pacific Northwest.

The 2004 and 1949 intercepts of linear fits to the time series of winter SFE/P values for each station were plotted against each other (Fig. 1b) to show the magnitude of changes during the 56-yr study period. A straight-line fit to all stations, in Fig. 1b, reveals that stations across the full range of initial SFE/P values have experienced remarkably uniform (slope ≈ 1) reductions in the fraction of precipitation falling as snow. The linear fit corresponds to an SFE/P decline of 9%

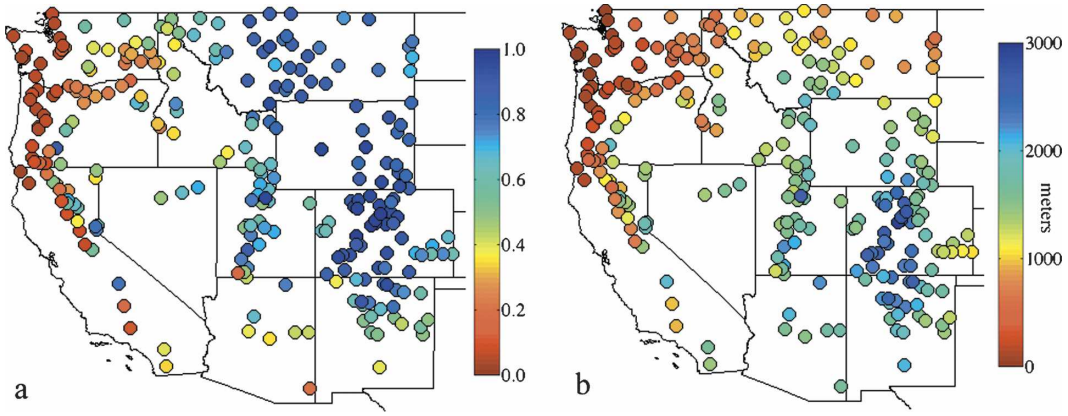

FIG. 2. (a) Mean winter (Nov–Mar) SFE/*P* values and (b) station elevations.

during the study period. In this paper, most trends will be discussed in terms of the difference of the linearly fitted values at the end and beginning of the study period; where trend strength is the focus (as opposed to trend magnitude), standard deviations are used (Figs. 1 and 3).

Long-term mean values of winter SFE/*P* (Fig. 2a) increase from west to east, responding to generally higher station elevations in the east (Fig. 2b), cooling with increasing latitude, and other geographic effects. Relatively little winter precipitation occurs as snow at many of the westernmost stations, which tend to be at lower altitudes and thus somewhat warmer in winter, whereas nearly all precipitation in the higher, cooler interior Rockies is snow.

Changes in SFE/*P* result from SFE changes that are disproportionate to changes in *P*. Figure 3 shows the WY1949–2004 trends (in terms of year-to-year standard deviations of the detrended time series) in winter *P* and SFE. The *P* trends (Fig. 3a) vary considerably in magnitude and sign over the spatial domain and are not generally in accord with the widespread pattern of SFE/*P* declines. Of the 48 stations with significant *P* trends, 15 also had significant trends in SFE/*P*. Of these, SFE/*P* trends were of the same sign as the *P* trends at 12 stations but, since *P* is inversely related to SFE/*P*, this means that in most cases *P* trends were not correlated with the SFE/*P* trends. In contrast, changes in SFE (Fig. 3b) more closely parallel the pattern of SFE/*P* trends shown in Fig. 1a. Of the 261 sites considered, 94 sites had significant SFE trends and 69 also had significant trends in SFE/*P*. Trends in SFE and SFE/*P* at 67 of these stations shared the same sign. In New England, Huntington et al. (2004) also found that SFE/*P* declines predominantly reflected trends toward smaller SFE.

The primary area where there have been disagreements between the signs of SFE trends (Fig. 3b) and SFE/*P* trends (Fig. 1a) is in the southern Rocky Mountains, in the southeastern portion of the study region. At most sites there, SFE increased in response to in-

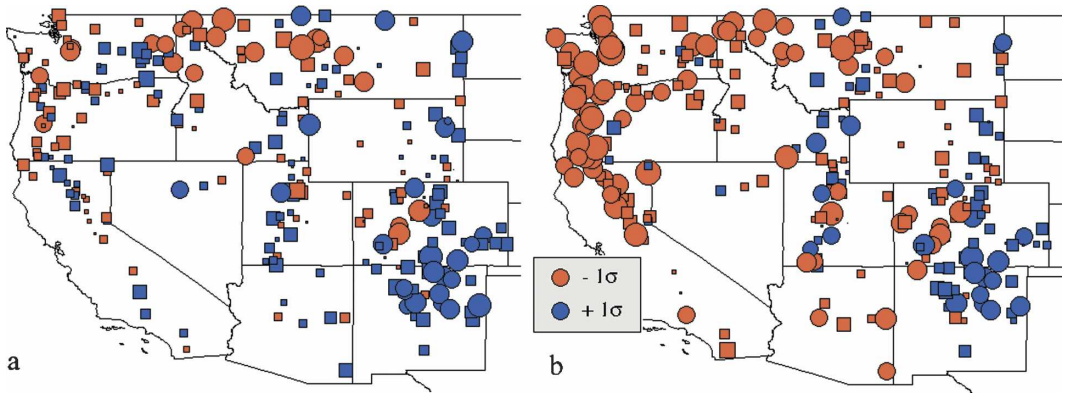

FIG. 3. The WY1949–2004 trends in winter (a) *P* and (b) SFE; significance of trends is shown by circles and squares as in Fig. 1a.

creasing *P*. At many of these sites, increases in SFE have not kept pace with *P*, and thus SFE/*P* ratios decreased. Relative within-season differences in when and how much precipitation and temperature changed (not shown) have played a secondary role in determining the SFE/*P* trends in this region. Precipitation in the southern Rockies has shifted into colder months, counteracting the warming trends and contributing to the mixed SFE/*P* trends there.

To further clarify the relationships between the trends in SFE/*P* and trends in SFE and *P*, Figs. 4a and 4b show trend magnitudes plotted against each other, with stations exhibiting significant SFE trends plotted as squares. Aside from a few sites that experienced large reductions in *P*, changes in SFE/*P* have not been well correlated with changes in *P* (Fig. 4a). Notably, decreases in *P* have generally coincided with *decreases in* SFE/*P* and increases in *P* have been associated with either decreases or increases in SFE/*P*, depending on location. Reductions in SFE have generally coincided with reductions in SFE/*P*, and some increases in SFE have coincided with increases in SFE/*P*, although the relation is not simple or linear (Fig. 4b).

The weak correlation between trends in SFE/*P* and trends in *P* is to be expected. If no factors other than trends in *P* influenced the ratio SFE/*P*, any trend in *P* should have produced a corresponding trend in SFE such that the ratio SFE/*P* showed no trend. That is, a trend in *P* should produce a trend in SFE equal to the initial value of SFE/*P* (i.e., the 1949 intercept of the linear fit) multiplied by the change in *P*. If the observed trend in SFE is less than this value as a result of influences other than *P*, then SFE/*P* decreases; if greater, it increases. This relationship is shown in Fig. 4c, where the observed trend in SFE at each station has been plotted against the expected SFE trend due solely to the trend in *P*. The symbols differ based on whether the observed trend in the ratio SFE/*P* was positive or negative. If no factors other than *P* had influenced SFE/*P*, all points would fall on the one-to-one line.

For the ratio SFE/*P* to have changed, then, some factor other than *P* must have influenced SFE at sites throughout the West. The next section discusses the role of temperature in producing SFE trends and distinguishes contributions to the trends due to precipitation changes from those due to temperature changes.

b. Temperature dependence

Several studies have linked declining snowpacks and earlier runoffs in the West to increasing temperatures (Dettinger and Cayan 1995; Cayan et al. 2001; Hamlet et al. 2005; Mote et al. 2005; Regonda et al. 2005; Stewart et al. 2005). The present analysis suggests that,

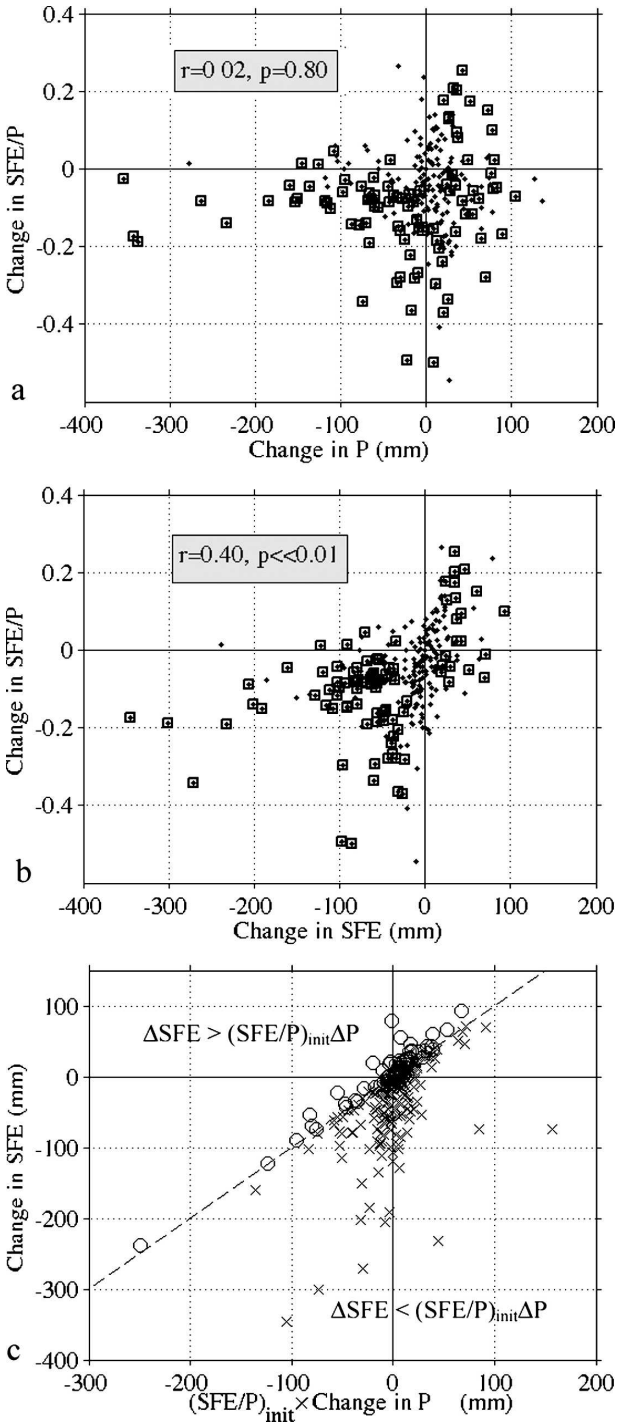

FIG. 4. (a) WY1949–2004 changes in winter SFE/*P* vs changes in winter *P*, with significant SFE/*P* trends highlighted with squares. (b) Changes in SFE/*P* vs changes in SFE. (c) Observed SFE changes vs SFE changes due solely to changes in *P*. Sites above the one-to-one line had increasing SFE/*P* (circles); at sites below the line, the ratio decreased (x's).

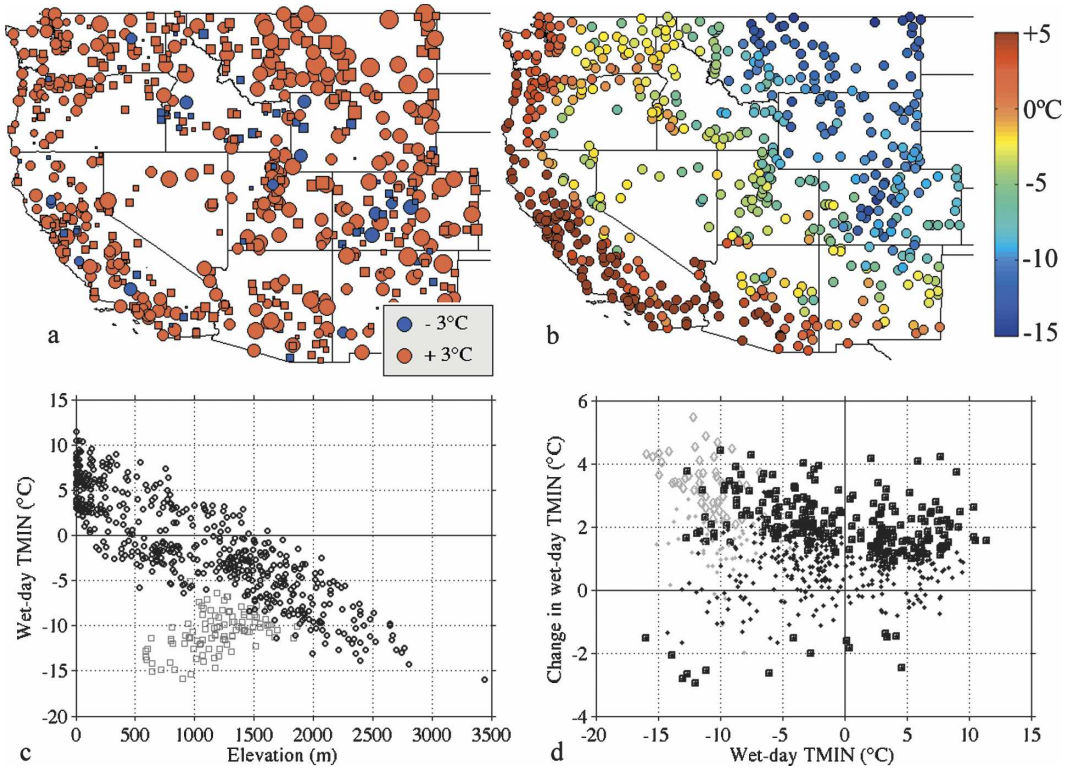

FIG. 5. (a) Trends in winter-mean daily-minimum wet-day air temperatures for 1949–2004. Symbol size is proportional to trend amount; circles indicate significant ($p < 0.05$) trends, squares indicate less significant trends. (b) Winter-mean wet-day minimum temperatures (TMINw). (c) TMINw vs station elevation. Great Plains stations are represented by gray squares. (d) Trends in TMINw vs mean TMINw, with significant trends highlighted as squares. Great Plains stations are identified in gray, with significant trends as diamonds.

among other possible mechanisms, warming has contributed to these changes by increasing the temperature during precipitation events, thus reducing the amount of snow deposited. To understand the relevant temperature changes, Fig. 5a shows trends in winter-mean wet-day minimum-daily temperatures. Wet-day TMINs have generally warmed more than have wet-day TMAXs (not shown), with average (over western U.S. stations) increases of +1.4°C and +1.0°C between 1949 and 2004, respectively (cf. Karl et al. 1993). Trends in dry-day TMAX and TMIN (not shown) have been similar in magnitude and spatial distribution to the wet-day trends. The remainder of this analysis will focus on winter (November–March) wet-day minimum temperatures (TMINw).

Long-term mean TMINw values are mapped in Fig. 5b. A clear southwest–northeast gradient is apparent in contrast to the northwest–southeast gradient in station elevations shown in Fig. 2b. Part of the reason for this is that Fig. 2b includes only stations from the precipitation–snowfall dataset, while Fig. 5b shows the larger set of temperature stations. Most stations in the warm Southwest did not have enough snowfall to qualify for the precipitation–snowfall dataset, so these warm stations, which are included in the temperature dataset, yield a more accentuated SW–NE pattern. Also, the Great Plains (GP) stations of Montana, Wyoming, and eastern Colorado are distinctly colder than other stations at comparable elevations and latitudes, further contributing to the SW–NE pattern in Fig. 5b. The anomalously cold temperatures of the GP stations are very apparent when mean TMINw values for each station are plotted against station elevations (Fig. 5c). In general, Fig. 5c demonstrates a clear-cut relationship between TMINw and elevation, with the spread of temperatures at a given elevation associated primarily with a spread of latitudes. However, the GP stations (distinguishable by light gray squares) show quite different behavior, with an inverted lapse rate and much colder temperatures.

Although some of the GP stations have had the largest warmings in the West (Fig. 5a), they are also among the coldest sites in the West (Figs. 5b and 5c) and have exhibited correspondingly little change in SFE/*P* to date. This tendency for colder stations to experience larger warmings holds for non-GP stations as well,

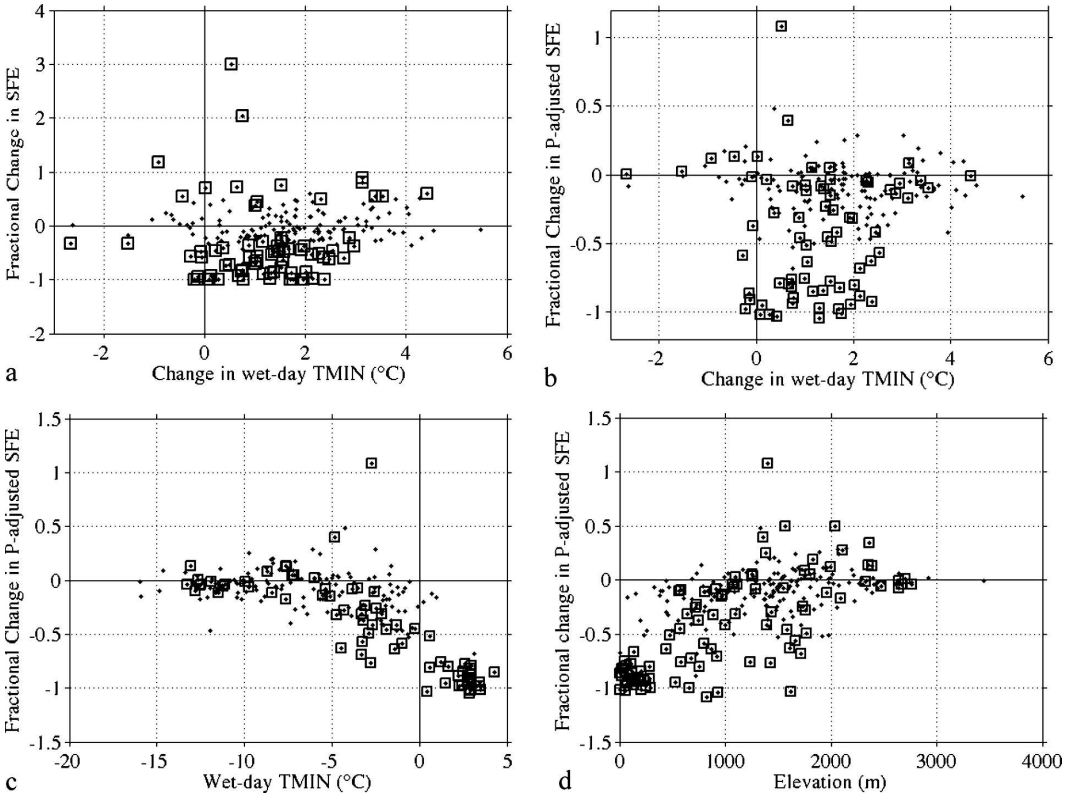

FIG. 6. (a) Fractional changes in SFE vs changes in TMINw over the period 1949–2004. (b) Fractional changes in precipitation-adjusted SFE vs trends in TMINw. (c) Fractional changes in precipitation-adjusted SFE vs TMINw. (d) Fractional change in precipitation-adjusted SFE vs station elevation. (a)–(d) Stations with statistically significant ($p < 0.05$) trends SPE are highlighted with squares.

though less dramatically. Figure 5d shows trends in TMINw plotted against mean TMINw, with significant trends highlighted, and significant GP trends identified as gray diamonds. Though the GP stations stand out as some of the coldest and most warmed in the West, many of the coldest non-GP stations have also warmed more than other, warmer non-GP sites. A total of 79% of the non-GP stations that had significant TMINw trends and that warmed more than +3°C had mean TMINw values less than 0°C; 70% of these had mean TMINw less than −5°C. In comparison, for non-GP stations with significant TMINw trends that warmed *less* than +3°C, these values were 47% and 40%, respectively.

To understand how these temperature changes have affected snowfall, fractional changes in SFE, expressed as the ratio of record-length SFE change to the initial SFE value (i.e., the 1949 intercept of the linear fit to the SFE time series) at each station, are plotted against the TMINw changes in Fig. 6a. Most stations with moderate TMINw changes experienced reductions in SFE. The outliers with large fractional SFE increases correspond to sites that had very little initial snowfall and that experienced very small increases in snowfall. Many sites lost most of their snowfall over the course of the 56-yr study period. However, at stations where TMINw warmed by more than about +3°C, SFE changed relatively little (increasing in most cases). This is a result of the very cold conditions at sites that experienced larger warmings (Fig. 5d) and is discussed further below.

To distinguish between the effects on SFE of trends in *P* and trends in TMINw, Fig. 6b shows an analog of Fig. 6a in which the changes in SFE have been adjusted to remove the influence of any *P* trend at each site. This was accomplished by subtracting the first-order effect of the precipitation trend at each station from the station's SFE trend. This first-order precipitation correction was estimated as the product of the *P* trend magnitude and the long-term mean of SFE/*P*. Earlier, the *initial* value of SFE/*P* was used to calculate the expected change in SFE/P due to *P* trends in the absence of other factors. Here, the use of the record-length mean of SFE/*P* is necessary because, as indicated by Fig. 4c, other factors have been influencing SFE/*P*. The SFE/*P* ratio has thus been changing over the course of

the record, and the record-length mean must be used to calculate a first-order approximation to the changes in SFE/*P* due to *P* trends. The assumption that changes in SFE due to changes in *P* can be removed in this manner is a simplification, but as will be shown, a useful one.

Once adjusted for *P* trends, it is even clearer (than in Fig. 6a) that the most significant reductions in SFE have occurred at sites that experienced moderate (<3°C) TMINw warming (Fig. 6b). The reason that smaller temperature changes resulted in the largest SFE declines is clear when viewed another way: Fig. 6c shows the *P*-adjusted SFE changes plotted against long-term mean November–March TMINw values at each site. The largest SFE reductions occurred at the warmest locations (TMINw > −5°C), where temperatures were closer to freezing and warming by even a small amount was enough to have a substantial impact. Because mean TMINw values are strongly related to elevation (Fig. 5c), *P*-adjusted SFE trends (Fig. 6d) are as well. Most *P*-adjusted SFE reductions occurred at sites with elevations below 2000 m, corresponding to the warmest temperatures in Fig. 6c. The few stations that exhibited appreciable fractional increases were largely located above about 1200 m and experienced relatively little snowfall; hence, small positive trends produced large fractional increases. At sites with significant winter SFE trends, the average *P*-adjusted winter SFE reduction was 51 mm over the 56-yr study period. Averaged over all sites, the reduction was 26 mm.

As noted above, the relationship between TMINw changes and the long-term mean wet-day winter temperatures (Fig. 5d) explains another feature evident in Figs. 6a and 6b, the very small SFE changes at sites that have warmed by more than +3°C. The stations that warmed this much tended to be among the coldest stations, with long-term November–March mean TMINw values less than −5°C. In these cold settings, even the largest warmings in the West—more than +4°C—were apparently not sufficient to yield significant SFE reductions.

Since mean TMINw and, to a lesser degree, trends in TMINw exhibit regional patterns, Figs. 6b and 6c also were plotted separately for individual regions, splitting the study domain into east–west, north–south, and northwest–southeast halves to test for effects of continentality, latitude, and elevation (Fig. 2a), respectively. In all three cases, the patterns corresponding to the halves showed considerable overlap and the relationships were consistent with those in Figs. 6b and 6c, indicating that *P*-adjusted SFE trends were not aliased artifacts of continentality, altitude, or elevation dependencies, but rather were driven by temperature trends.

The geographic pattern of *P*-adjusted SFE trends resulting from the TMINw trends (Fig. 5a) and mean TMINw (Fig. 5b) is shown in Fig. 7. The *P*-adjusted SFE was reduced at 75% of all stations in the West, with 20% of all stations experiencing reductions of greater than one-half of their initial snowfall. The largest reductions occurred at stations in the coastal Pacific Northwest. Although these sites experienced only moderate warming (Fig. 5a), they were also among the warmest sites (Fig. 5b) and therefore had the largest fractional SFE reductions, consistent with the relationships revealed by Figs. 6b and 6c. Sites in central and northern California received, on average, considerably more snow than any other region, and in terms of magnitude, they showed the largest snowfall reductions in the West.

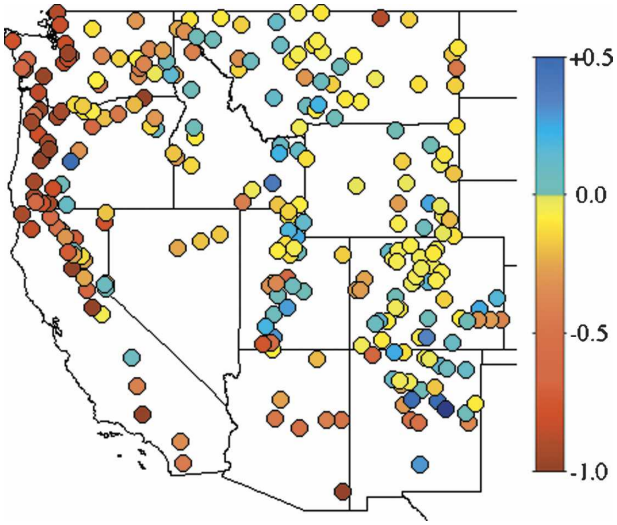

FIG. 7. WY1949–2004 fractional change in winter snowfall water equivalent after removing the effects of trends in precipitation. A total of 75% of stations have experienced snowfall reductions as a result of widespread warming (Fig. 5a).

The pattern in Fig. 7 therefore results from the patterns in Figs. 5a and 5b, which are in turn dependent on elevation, latitude, and other geographic factors responsible for temperature patterns. Another key factor was the relationship between warming and mean wet-day daily-minimum temperatures: the sites that warmed the most tended to have the coldest mean temperatures. The relationships expressed in Figs. 6b and 6c are fundamental in determining the change in snowfall, and they hold throughout the study region.

c. *Monthly patterns*

Mapping trend magnitudes for SFE/*P* by month (Fig. 8) reveals that the most widespread declines in snowfall fractions occurred in March, with declines spanning the western United States. Important declines in SFE/*P*

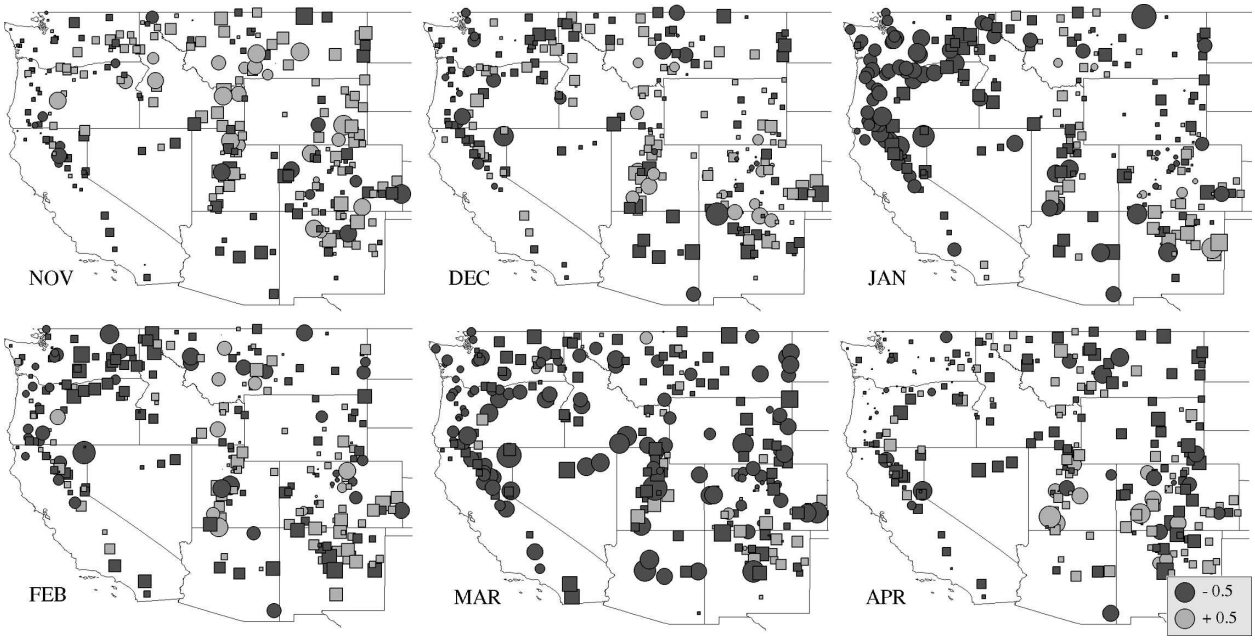

FIG. 8. Trend amounts for monthly averaged SFE/*P*. January and March have shown the largest reductions in response to warming trends (Fig. 9).

also occurred in January along the West Coast (in stations associated with the Sierra Nevada and the Pacific Northwest). On average, January is the top snow-producing month at most of the Sierra Nevada and Pacific Northwest stations, whereas March is a major snow-producing month in the Rockies. Thus, the declines are of considerable concern.

The seasonality of the monthly SFE/*P* changes echoes the monthly changes in TMINw (Fig. 9). In particular, January and March have warmed most significantly across the West. Monthly patterns of TMAXw trends were very similar to those in Fig. 9, though with smaller increases in general. In addition, dry days have warmed by about the same amount as wet days during the study

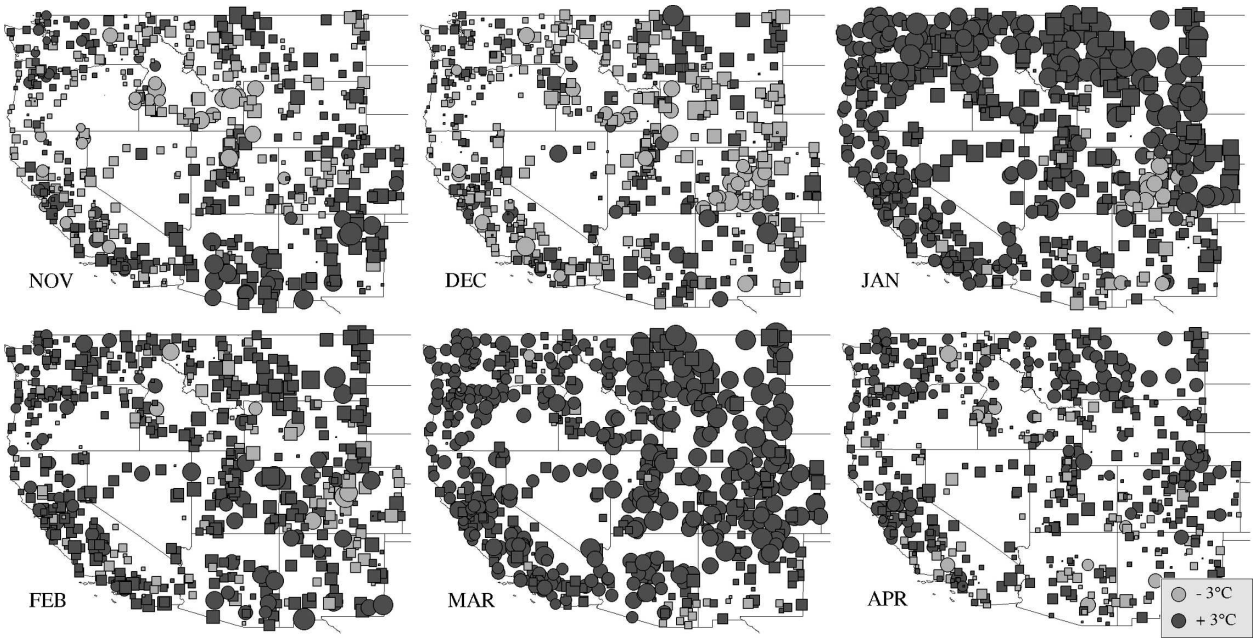

FIG. 9. Trend amounts for monthly averaged TMINw. January and March have had particularly widespread warming trends.

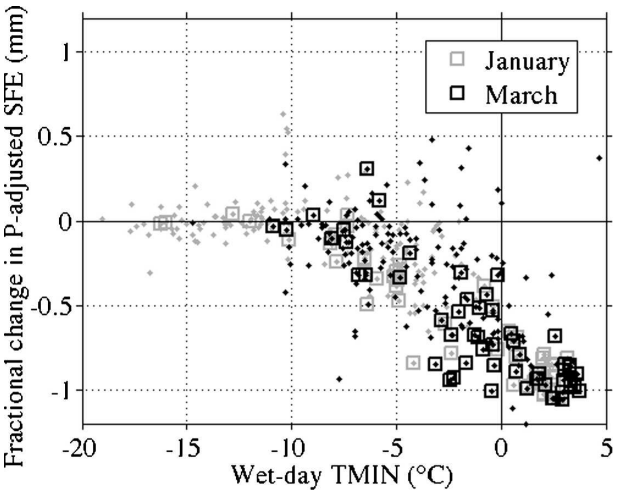

FIG. 10. Fractional precipitation-adjusted SFE changes vs mean TMINw for January and March. Note the greater number of very cold (TMINw < -10°C) stations in January compared to March, which resulted in less widespread SFE/*P* declines in January. Statistically significant ($p < 0.05$) trends are highlighted with squares.

period, with very nearly the same monthly patterns (not shown).

Monthly trend patterns in *P* were generally less organized than the January and March temperature trends, with net reductions in *P* over the course of the study period in the northern Rockies and Cascades in December, January, and February, and net increases in the southern Rockies in most months, leading to the winter-average pattern (Fig. 3a).

Three conditions must be met for temperature-driven SFE reduction to occur: 1) snowfall must have occurred in the early portion of the study period, 2) warming must take place over the study period, and 3) the mean temperature must be warm enough for warming to have an effect. The fraction of stations satisfying each of these conditions varied seasonally, with corresponding influences on the prevalence of *P*-adjusted snowfall declines and the SFE/*P* trend patterns (Fig. 8). Historically, snowfall occurred at most stations during all winter months, with a sharp drop in the number of stations that normally received snow in springtime. On average, the largest percentages of stations experienced warming in January and March (about 90% and 96%, respectively), and the smallest percentage of stations were warm enough for warming to affect SFE (historical mean TMINw > -5°C) in January (38%). This last factor explains why similar warming patterns in January and March (Fig. 9) resulted in different SFE/*P* responses (Fig. 8). January TMINw values were too cold at higher elevations for the warming to affect SFE (Fig. 10). In March, most stations were warm enough for the broad warming trends to yield broad SFE/*P* declines.

Although January SFE/*P* ratio reductions were not as widespread as those in March, the average January SFE declines were slightly greater. Averaged over *all* stations, the *P*-adjusted SFE reductions were 10 mm in January and 8 mm in March, with smaller reductions during the other winter months. These reductions amounted, on average, to 14% and 9%, respectively, of winter SFE totals. The larger January SFE declines reflect the fact that West Coast stations receive much more *P* (and, at moderate elevations, more SFE) than interior stations, with peak *P* and SFE in January. The combination of large (historical mean) snowfall, significant warming, and sufficiently warm mean January temperatures at these sites resulted in the largest monthly SFE declines in the West occurring at near-coastal sites in January.

d. Climate variability

So far, only linear trends have been examined. Using an empirical orthogonal function (EOF) analysis, the temporal evolution of the system can be examined in more detail and farther back in time. Figures 11 and 12 show the first modes and associated amplitude time series from six different EOF analyses. To produce these results, the TMINw and SFE/*P* time series were extended back first to WY1930 and then to WY1920. In the WY1930–2004 series, 91 precipitation–snowfall stations and 330 temperature stations satisfied the completeness criteria; in the WY1920–2004 series, there were 45 and 251 stations, respectively. The time series at all stations were standardized to have zero mean and a standard deviation of one over each of the time intervals analyzed. The EOF analysis was then applied to these four datasets as well as to the original WY1949–2004 datasets.

For each of the three time periods, the first EOFs of November–March average TMINw are everywhere positively weighted (except for one station in Colorado), capturing variations shared by all stations. In each analysis, the first EOF explains around 40% of the overall TMINw variance (Fig. 11, top). The first EOFs of SFE/*P* explain around 20% of the SFE/*P* variance, with most stations varying in unison but a few in opposition (Fig. 11, bottom). Despite the much sparser datasets for the longer analysis periods, Fig. 11 shows that the same basic patterns dominated all three analyses. Indeed, when the first-EOF amplitudes for all three are plotted on top of each other, they agree remarkably well (Fig. 12), with correlation coefficients for overlapping time periods greater than 0.94 in all cases. The first-EOF amplitudes for TMINw and SFE/*P* are also

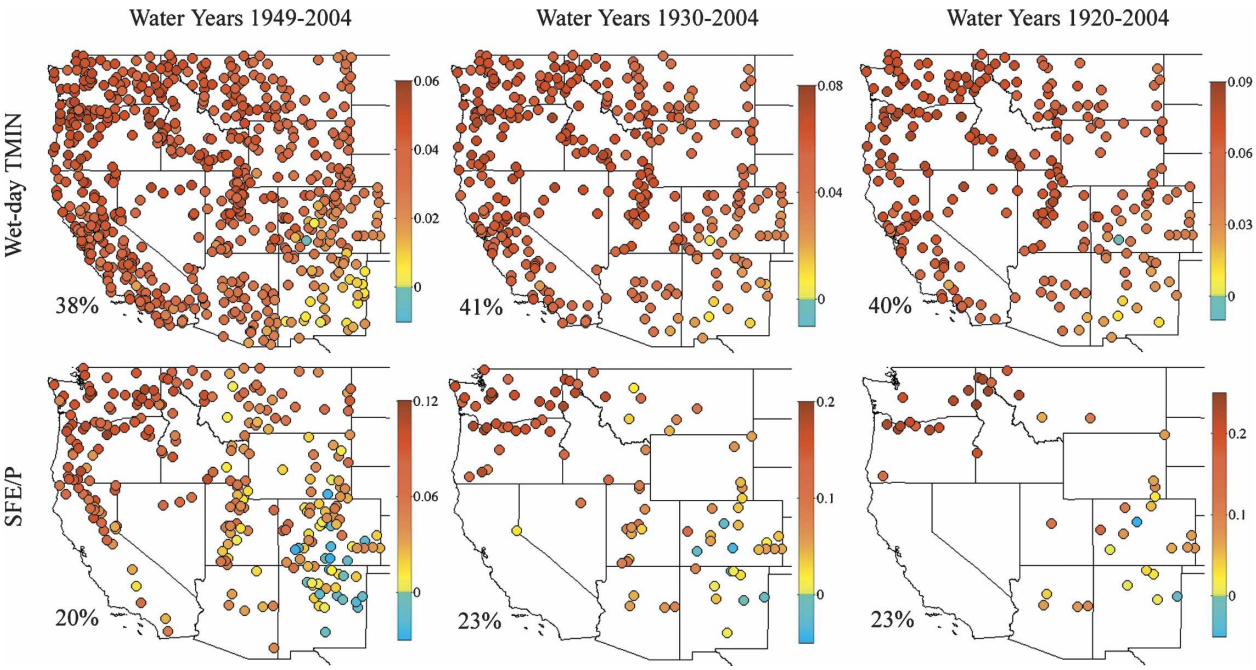

FIG. 11. First EOFs for six time series: (top) TMINw and (bottom) SFE/*P* for the periods WY1949–2004, WY1930–2004, and WY1920–2004. Percent of overall variance explained is in lower left of each panel.

strongly anticorrelated, with correlations more negative than −0.87 for all three time periods. Thus, on time scales from annual to long-term trends, temperature increases produce decreases in SFE/*P*.

The first EOFs are of particular interest because they represent spatially coherent variations on the largest scale, a scale that characterizes the trends presented above. The lower-order EOFs reflect smaller spatial scales, such as spatial dipoles, and are not presented here. The first EOF amplitudes in Fig. 12 are strongly related to the time series of TMINw and SFE/*P* averaged over all stations (not shown) and to each other. The correlations between TMINw first EOF amplitudes and the time series of all-station-average TMINw are 0.99 for all three time periods. The corresponding correlations for SFE/*P* are 0.86 for 1920–2004, 0.89 for 1930–2004, and 0.92 for 1949–2004.

Also shown in Fig. 12 are smoothed versions of the first EOF amplitudes. These were generated from the annual EOF amplitudes using a low-pass filter with a 10-yr cutoff period (Mann 2004). While the smoothed versions were generated for the full time period corresponding to each EOF amplitude time series, the smoothed versions shown in each period in Fig. 12 are the smoothings from the richest datasets with temporal coverage appropriate for the 10-yr smoothing period used. That is, the smooth solid line from 1954 to 2004 is the filtered version of the first EOF amplitude from the 1949–2004 dataset, the smooth dashed line from 1935 to 1954 is from the 1930–2004 EOF analysis, and the smooth dotted line from 1920 to 1935 is from the 1920–2004 analysis. This approach provides an optimal representation of low-frequency behavior for each period of the record, as more stations came online.

The positive temperature trend and the shift from snowfall to rainfall during WY1949–2004 presented earlier are evident in the smoothed amplitudes (Fig. 12). It also appears that the changes composing the WY1949–2004 trends occurred largely in the 1950s and after the late 1970s.

One reason for extending the analysis back to 1920 was to determine whether the trends presented here are artifacts of the WY1949–2004 study period that supplied most of the data for the analyses. That widespread meteorological observations did not become available until 1948 is an unfortunate constraint on the present analysis. The winter of WY1949 was particularly cold in the historical record, and SFE/*P* ratios were correspondingly high. Also, during approximately the first half of the 1949–2004 study period, the Pacific decadal oscillation (PDO; Mantua et al. 1997) was in its cool phase, after which it transitioned to a warm phase that persisted throughout most of the second half of the study period (more recently still, the PDO may have reentered its cool phase, though its present status is not clear).

Though the amplitudes become more uncertain as fewer stations were existent farther back in time, it does

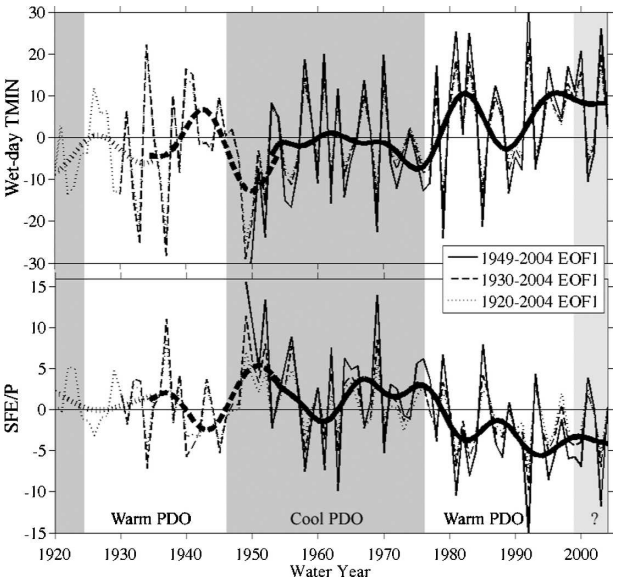

FIG. 12. First EOF amplitudes representing spatially broad patterns of (top) variability in winter wet-day minimum temperature and (bottom) fraction of winter precipitation falling as snow, with PDO phases indicated. These amplitudes correspond to the spatial loading patterns in Fig. 11. The thick, wavy lines are low-pass-filtered versions of each amplitude. The portion of the low-pass curve that best describes a given period is used for that period. See text for further explanation.

appear that a portion of the trends detected since 1949 may be attributable to low-frequency climate variability, since the 1947–1976 cool phase was characterized by cooler temperatures and higher SFE/*P* ratios than both the 1925–1946 and the 1977–1998 warm phases. These conclusions were also borne out by a separate examination of the all-station means (using the 1920–2004 dataset) of TMINw and SFE/*P* (Table 1).

However, the PDO warm phase lasting from about 1925 through 1946 was characterized by lower temperatures and higher SFE/*P* values than the most recent 1977–1998 PDO warm phase (Table 1), suggesting that the trends reported here are at least partially attributable to still longer-term climate shifts. Indeed, when the entire analysis presented in sections 3a and 3b was repeated using the 1930–2004 data and again using the 1920–2004 data, although the plots contained fewer data points, the resulting trend maps and plots were essentially unchanged.

TABLE 1. Mean (over all stations in the 1994–2004 dataset) TMINw and SFE/*P* for three phases of the PDO. The differences between the two warm phases are of the same order of magnitude and in the same direction as the overall WY1920–2004 trends. Also shown are the differences between the two warm phases, as well as the mean record-length trend.

	TMINw (°C)	SFE/*P*
WY1925–1946 (warm)	−2.8	0.56
WY1947–1976 (cool)	−3.0	0.57
WY1977–1998 (warm)	−2.4	0.54
Warm-phase difference	+0.4	−0.02
WY1920–2004 trend	+1.1	−0.06

4. Conclusions

Observations over the last half-century have demonstrated that, across a broad region of mountainous western North America, spring snow accumulation has declined (e.g., Mote et al. 2005) and snowmelt has come earlier in the year (e.g., Stewart et al. 2005). The present study provides supporting evidence for changes in one of the primary mechanisms involved: temperatures have warmed during winter and early spring storms, and, consequently, the fraction of precipitation that fell as snow declined while the fraction that fell as rain increased.

During the period WY1949–2004, significant changes in November–March seasonal total snowfall water equivalent (SFE) were much more common than changes in seasonal total precipitation, and most of the significant changes in SFE were reductions unrelated to changes in total precipitation. The largest reductions were shifts from snowfall to rainfall driven by warming and occurred at relatively warm, low to moderate elevations (Fig. 6).

Warming trends were widespread across the western United States. Importantly, wet days have warmed about slightly more than dry days during winter and spring over the study period. However, the sites that warmed most tended to have relatively cold climatologies. As a result, some of the largest warming trends in the West (>4°C) did not cause shifts in precipitation form (from snow to rain) because, despite the warming, temperatures remained well below freezing. The largest shifts from snowfall to rainfall actually occurred at sites that warmed less (from 0° to +3°C), because these sites had mean temperatures warm enough that moderate warming was sufficient to impact the precipitation form (Fig. 6c).

In summary, the mean temperatures (Fig. 6c) and the magnitude and sign of the surface temperature trends (Fig. 6b) were the fundamental determinants of the amount of precipitation shifting from snow to rain at each site. Although mean temperatures and, to a lesser extent, temperature trends exhibit regional patterns, it was verified that the temperature dependencies expressed in Figs. 6b and 6c hold throughout the study region; that is, they are not simply aliased regional patterns. This fact, combined with the widespread nature

of the warming trends (Fig. 5a) and the strong elevational dependence of mean temperatures (Fig. 5c), suggests that the east–west pattern of fractional precipitation-adjusted snowfall reduction of Fig. 7 is primarily a reflection of station elevation (Fig. 2a) and is not indicative of some other regional control on snowfall reductions. Thus, the snowfall declines seen at the cooperative stations included in the present study are probably also occurring at most other (as yet undocumented) sufficiently warm, low- to moderate-elevation sites in the West.

We found that while PDO fluctuations may have influenced wet-day temperatures and snowfall fractions at the interdecadal time scale, it also appears that longer-term changes have been occurring. This result is consistent with recent findings of reduced spring snowpack by Mote et al. (2005) and advanced snowmelt runoff by Stewart et al. (2004), who suggest that these changes can only be partially explained by fluctuations in PDO, with another portion of the variability that may be a response to broader-scale anthropogenic warming.

If warming trends across the western United States continue, as projected in response to increasing greenhouse gas concentrations in the atmosphere (IPCC 2001), the snowfall fraction of precipitation is likely to continue to decline. More warming may be expected to produce rightward and downward drifts of the points in Fig. 6c. When a station's mean November–March wet-day minimum temperature rises above about −5°C in that figure, the station's snowfall amounts begin to respond to the warming trends that bring temperatures closer to freezing, and continued warming shifts precipitation from snow to rain. Figure 5d indicates that the coldest stations in Fig. 6c have been warming more quickly than the warmer stations. Month-by-month trend analyses showed that the effect of future warming on snowfall amounts will depend critically on warming in specific precipitation-rich months (e.g., January and March, to date), yielding the largest impacts when the greatest warming coincides with the greatest (historical) snowfall amounts and suitably warm mean temperatures. Warming during December–March would have the largest impact on snow deposition, while warming in April through June will be more strongly expressed as accelerations of snowpack melting like those projected by Stewart et al. (2004).

If warming continues and raises the mean winter wet-day minimum temperatures in more of the West above about −5°C, snowfall declines (and rainfall increases), combined with earlier melting of the remaining accumulations of snowpack, will diminish the West's natural freshwater storage capacity. The shift from snowfall to rainfall also may be expected to increase risks of winter and spring flooding in many settings. The combination of greater flood risk and reduced natural storage threatens to exacerbate the tension between flood control and storage priorities that many western reservoir managers face. Better understanding of how flood risks will change, of the atmospheric conditions that control precipitation form, and of possible trends in those conditions are needed to project and accommodate future changes in the West's water supplies.

Acknowledgments. Thanks to Alexander Gershunov and Emelia Bainto for assistance in retrieving and processing SOD data, and to Kelly Redmond and Ken Kunkel for feedback and advice concerning COOP observations. Support for NK came from the National Research Council Research Associateship Program at the USGS, the CALFED Ecosystem Restoration Program (project ERP-02-P38), and the California Energy Commission's Public Interest Energy Research Program (PIER) through the California Climate Change Center (CCCC) at the Scripps Institution of Oceanography. Support for DRC was from the NOAA Office of Global Programs through the California Applications Program, the Department of Energy, and the CEC PIER CCCC. MDD's support was from the USGS Hydroclimatology Program and the CEC PIER CCCC.

REFERENCES

Cayan, D. R., S. A. Kammerdiener, M. D. Dettinger, J. M. Caprio, and D. H. Peterson, 2001: Changes in the onset of spring in the western United States. *Bull. Amer. Meteor. Soc.,* **82,** 399–415.

Dettinger, M. D., and D. R. Cayan, 1995: Large-scale atmospheric forcing of recent trends toward early snowmelt in California. *J. Climate,* **8,** 606–623.

——, M. Ghil, and C. L. Keppenne, 1995: Interannual and interdecadal variability of United States surface-air temperatures, 1910–1987. *Climatic Change,* **31,** 35–66.

——, D. R. Cayan, M. K. Meyer, and A. E. Jeton, 2004: Simulated hydrologic responses to climate variations and change in the Merced, Carson, and American River basins, Sierra Nevada, California, 1900–2099. *Climatic Change,* **62,** 283–317.

Diaz, H. F., and R. G. Quayle, 1980: The climate of the United States since 1895—Spatial and temporal changes. *Mon. Wea. Rev.,* **108,** 249–266.

Easterling, D. R., T. R. Karl, E. H. Mason, P. Y. Hughes, and D. P. Bowman, 1996: United States Historical Climatology Network (U.S. HCN) monthly temperature and precipitation data. ORNL/CDIAC-87, NDP-019/R3, Carbon Dioxide Information Analysis Center, Oak Ridge National Laboratory, Oak Ridge, TN, 280 pp.

——, ——, J. H. Lawrimore, and S. A. Del Greco, 1999: United States Historical Climatology Network daily temperature, precipitation, and snow data for 1871–1997. ORNL/CDIAC-118, NDP-070, Carbon Dioxide Information Analysis Center,

Oak Ridge National Laboratory, Oak Ridge, TN, 84 pp. [Available online at ftp://ftp.ncdc.noaa.gov/pub/data/ushcn/daily/README.txt.]

Gleick, P. H., 1987: The development and testing of a water balance model for climate change impact assessment—Modeling the Sacramento Basin. *Water Resour. Res.,* **23,** 1049–1061.

Groisman, P. Y., and D. R. Legates, 1994: The accuracy of United States precipitation data. *Bull. Amer. Meteor. Soc.,* **75,** 215–227.

Hamlet, A. F., P. W. Mote, M. P. Clark, and D. P. Lettenmaier, 2005: Effects of temperature and precipitation variability on snowpack trends in the western United States. *J. Climate,* **18,** 4545–4561.

Huntington, T. G., G. A. Hodgkins, B. D. Keim, and R. W. Dudley, 2004: Changes in the proportion of precipitation occurring as snow in New England (1949–2000). *J. Climate,* **17,** 2626–2636.

McCarthy, J. J., O. F. Canziani, N. A. Leary, D. J. Dokken, and K. S. White, Eds., 2001: *Climate Change 2001: Impacts, Adaptation and Vulnerability.* Cambridge University Press, 1000 pp.

Karl, T. R., H. F. Diaz, and G. Kukla, 1988: Urbanization—Its detection and effect in the United States climate record. *J. Climate,* **1,** 1099–1123.

——, and Coauthors, 1993: A new perspective on recent global warming: Assymetric trends of daily maximum and minimum temperature. *Bull. Amer. Meteor. Soc.,* **74,** 1007–1023.

Kendall, M. G., 1938: A new measure of rank correlation. *Biometrika,* **30,** 81–93.

Knowles, N., and D. Cayan, 2004: Elevational dependence of projected hydrologic changes in the San Francisco estuary and watershed. *Climatic Change,* **62,** 319–336.

Lettenmaier, D. P., and T. Y. Gan, 1990: Hydrologic sensitivities of the Sacramento–San Joaquin River Basin, California, to global warming. *Water Resour. Res.,* **26,** 69–86.

Mann, M. E., 2004: On smoothing potentially non-stationary climate time series. *Geophys. Res. Lett.,* **31,** L07214, doi:10.1029/2004GL019569.

Mantua, N. J., S. R. Hare, Y. Zhang, J. M. Wallace, and R. C. Francis, 1997: A Pacific interdecadal climate oscillation with impacts on salmon production. *Bull. Amer. Meteor. Soc.,* **78,** 1069–1079.

Mote, P. W., 2003: Trends in snow water equivalent in the Pacific Northwest and their climatic causes. *Geophys. Res. Lett.,* **30,** 1601, doi:10.1029/2003GL017258.

——, A. F. Hamlet, M. P. Clark, and D. P. Lettenmaier, 2005: Declining mountain snowpack in western North America. *Bull. Amer. Meteor. Soc.,* **86,** 1–39.

National Weather Service, 1989: *Cooperative Station Observations. National Weather Service Observing Handbook,* No. 2, Observing Systems Branch, Office of Systems Operations, 94 pp. [Available online at http://weather.gov/om/coop/Publications/coophandbook2.pdf.]

Regonda, S., M. P. Clark, B. Rajagopalan, and J. Pitlick, 2005: Seasonal cycle shifts in hydroclimatology over the western United States. *J. Climate,* **18,** 372–384.

Roos, M., 1991: A trend of decreasing snowmelt runoff in northern California. *Proc. 59th Western Snow Conf.,* Juneau, AK, 29–36.

Stewart, I. T., D. R. Cayan, and M. D. Dettinger, 2004: Changes in snowmelt runoff timing in western North America under a 'business as usual' climate change scenario. *Climatic Change,* **62,** 217–232.

——, ——, and ——, 2005: Changes toward earlier streamflow timing across western North America. *J. Climate,* **18,** 1136–1155.

U.S. Department of Agriculture Weather Bureau, 1935: Instructions for cooperative observers. Circulars Band C, Instrument Division, eighth ed. W. B. 843, 33 pp.

Yang, D., B. E. Goodison, J. R. Metcalfe, V. S. Golubev, R. Bates, T. Pangburn, and C. L. Hanson, 1998: Accuracy of NWS 8" standard nonrecording precipitation gauge: Results and application of WMO intercomparison. *J. Atmos. Oceanic Technol.,* **15,** 54–68.